The EMBO Journal Vol.17 No.3 pp.635–647, 1998

Distinct functions of calmodulin are required for the uptake step of receptor-mediated endocytosis in yeast: the type I myosin Myo5p is one of the calmodulin targets

M.Isabel Geli, Andreas Wesp and Howard Riezman[1]

Biozentrum of the University of Basel, CH-4056 Basel, Switzerland

[1]Corresponding author
e-mail: riezman@ubaclu.unibas.ch

The uptake step of receptor-mediated endocytosis in yeast is dependent on the calcium binding protein calmodulin (Cmd1p). In order to understand the role that Cmd1p plays, a search was carried out for possible targets among the genes required for the internalization process. Co-immunoprecipitation, two-hybrid and overlay assays demonstrated that Cmd1p interacts with Myo5p, a type I unconventional myosin. Analysis of the endocytic phenotype and the Cmd1p–Myo5p interaction in thermosensitive *cmd1* mutants indicated that the Cmd1p–Myo5p interaction is required for endocytosis *in vivo*. However, the Cmd1p–Myo5p interaction requirement was partially overcome by deleting the calmodulin binding sites (IQ motifs) from Myo5p, suggesting that these motifs inhibit Myo5p function. Additionally, genetic and biochemical evidence obtained with a collection of *cmd1* mutant alleles strongly suggests that Cmd1p plays an additional role in the internalization step of receptor-mediated endocytosis in yeast.

Keywords: calmodulin/endocytosis/*Saccharomyces cerevisiae*/type I myosin

Introduction

Endocytosis is the process whereby eukaryotic cells internalize extracellular material as well as part of their own plasma membrane, facilitating uptake of nutrients, down-regulation of receptors and removal of damaged proteins from the cell surface. The development of assays that quantitatively measure receptor-mediated internalization in the yeast *Saccharomyces cerevisiae* has facilitated identification of many genes specifically required in this process (Riezman *et al*., 1996 and references therein). Analysis of these genes indicates that the actin cytoskeleton plays a fundamental role in the endocytic uptake in yeast. (Kübler and Riezman, 1993; Raths *et al*., 1993; Bénédetti *et al*., 1994; Kübler *et al*., 1994; Munn *et al*., 1995; Geli and Riezman, 1996; Wendland *et al*., 1996; Wesp *et al*., 1997; Tang *et al*., 1997). Even though the requirement for the actin cytoskeleton in endocytic uptake in animal cells has been a matter of discussion for a long time, evidence now suggests that it also plays a role in both clathrin-dependent and -independent endocytic pathways (Lamaze *et al*., 1997).

The Ca^{2+} sensor, calmodulin is one of the proteins that may play a fundamental role in the regulation of the cytoskeleton re-arrangements required to form an endocytic vesicle. Calmodulin has been implicated in regulating actin–actin, actin–myosin and actin–plasma membrane associations in many cell types including yeast (reviewed in Clore *et al*., 1993; Janmey, 1994; Ohya and Botstein, 1994a,b; James *et al*., 1995).

One single essential gene (*CMD1*) encodes calmodulin in *S.cerevisiae* (*CMD1*) (Davis *et al*., 1986). Previous work from our laboratory has demonstrated that calmodulin plays a fundamental role in endocytosis (Kübler *et al*., 1994). A temperature sensitive (ts) calmodulin mutant (*cmd1-1*) was completely blocked for α-factor internalization almost immediately upon shift to the restrictive temperature. The calmodulin requirement is apparently calcium independent because the ts mutant, *cmd1-3*, impaired in Ca^{2+} binding *in vitro* (Geiser *et al*., 1991), allowed wild type (wt) internalization kinetics (Kübler *et al*., 1994). In addition, some evidence of a role for calmodulin in the uptake step of endocytosis in mammalian cells also exists. Calmodulin has been purified from clathrin coated vesicles and was shown to interact with clathrin light-chain (Salisbury *et al*., 1980; Pley *et al*., 1995). Further, endocytosis of the cell surface IgM receptor in lymphoblastoid cells is sensitive to the calmodulin directed drug, Stelazine (Salisbury *et al*., 1980).

In order to further understand the actin- and calmodulin-dependent mechanism that functions in endocytic internalization in yeast, we searched for calmodulin targets among the proteins known to be required for this process. Specifically, we investigated the physical and functional interaction between calmodulin and the unconventional type I myosin, Myo5p. Type I myosins are ubiquitous actin/ATP-dependent molecular motors that bear a short, positively-charged C-terminal domain that can bind acidic phospholipids and cellular membranes (reviewed in Korn and Hammer, 1990; Pollard *et al*., 1991; Tan *et al*., 1992; Mooseker and Cheney, 1995; Titus, 1997). Two functionally redundant genes encode for type I myosins in yeast: *MYO3* and *MYO5* (Goodson and Spudich, 1995; Geli and Riezman, 1996; Goodson *et al*., 1996). Myo5p seems to play a major role in endocytosis, because deletion of *MYO5* (but not *MYO3*) caused a strong defect in α-factor internalization at elevated temperatures. Deletion of both genes caused a synthetically lethal phenotype that was complemented with a ts *myo5* allele (*myo5-1*). The ts strain was completely blocked for internalization of α-factor and its receptor, Ste2p, at the restrictive temperature (Geli and Riezman, 1996). The role of type I myosin in the internalization step of endocytosis is not restricted to yeast. A strong defect in pinocytic uptake has also been described for *Dictyostelium* type I myosin mutants (Novak *et al*., 1995; Jung *et al*., 1996).

All myosins described thus far bear at least one IQ

consensus motif (IQXXXRXXXXR) at the neck between the motor head and the tail domains. The IQ motifs can constitute binding sites for small EF-hand-containing proteins, which are thought to work as myosin light-chains and may confer Ca^{2+} sensitivity to myosin regulation. Many vertebrate type I myosins co-purify with calmodulin and interestingly, maximal binding of calmodulin is generally achieved in the absence of Ca^{2+}, in contrast to what is seen for many other calmodulin-activated enzymes (Wolenski, 1995).

Whether calmodulin is required for type I myosin function *in vivo*, and whether it regulates myosin activity in a Ca^{2+}-dependent manner, is still a matter of debate since this subject has mainly been addressed *in vitro* and the results obtained seem to vary depending on the myosin studied and the assay used to monitor its activity (Wolenski, 1995 and references therein). In addition, some type I myosins do not seem to bind calmodulin, and their Mg^{2+}-ATPase is fully active in the absence of light-chains (Maruta, 1978).

Here, we present evidence showing that calmodulin interacts with the type I myosin, Myo5p. Analysis of a collection of ts *cmd1* mutants for their endocytic phenotype and their ability to bind Myo5p strongly indicates that Cmd1p–Myo5p interaction is required to drive endocytic internalization. This requirement is partially overcome by deletion of the calmodulin binding sites of Myo5p, suggesting that the IQ motifs may overlap with a Myo5p auto-inhibitory domain. In addition, we present genetic evidence suggesting that calmodulin also fulfills a Myo5p-independent function in the uptake step of receptor-mediated endocytosis in yeast.

Results

Myo5p associates with Cmd1p

Since Myo5p and Cmd1p are both required for the uptake step of receptor-mediated endocytosis and interaction between calmodulin and type I myosins have been previously described in vertebrate systems, we decided to investigate whether Cmd1p and Myo5p physically interact and whether this interaction is relevant for their endocytic function *in vivo*.

To test for a physical interaction between Cmd1p and Myo5p, we raised a polyclonal serum against Cmd1p and we tagged Myo5p with a myc epitope for detection in co-immunoprecipitation experiments. The specificity of the α-Cmd1p antibody was confirmed by immunoblotting, comparing extracts from yeast expressing either wild type (wt) Cmd1p or a mutant calmodulin with slower SDS–PAGE mobility (Cmd1-228p) (Figure 1A). Additionally, a difference in apparent molecular weight of the recognized band was observed in wt extracts depending on the presence of 100 mM EGTA or 100 mM $CaCl_2$ in the SDS–PAGE loading buffer (Brockerhoff, 1992) (Figure 1A). The myc-tagged *MYO5* was subcloned in a 2μ plasmid to create pA12myc*MYO5* and transformed in a strain deleted for the genomic *MYO5* (strain RH3976). As a control, the same strain was transformed with a plasmid bearing a non-tagged *MYO5*. Total protein extracts from each strain were separated by SDS–PAGE and immunoblotted using the α-myc monoclonal antibody (9E10). A band of the expected molecular weight (137 kDa) was detected exclusively in the extract from the strain expressing the myc-tagged Myo5p (Figure 1A). 2μ and centromeric plasmids bearing myc-tagged *MYO5* fully complemented a *myo5*Δ strain by the following criteria: (i) they supported wt growth when combined with a *MYO3* deletion; (ii) they supported α-factor uptake with wt kinetics in the presence or absence of Myo3p (data not shown).

A native extract enriched for Myo5p was used for immunoprecipitation with the α-Cmd1p serum. Since maximal calmodulin binding has been observed in the absence of Ca^{2+} for most type I myosins, the whole procedure was performed in the presence of 1 mM EGTA.

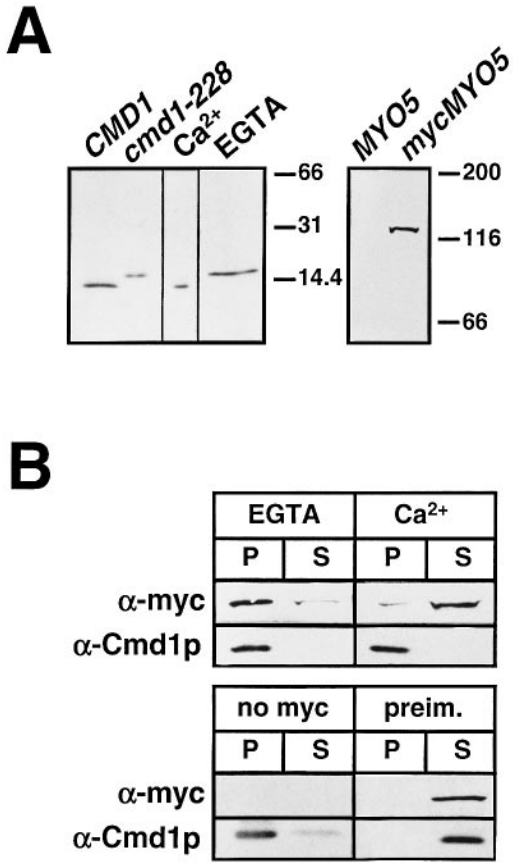

Fig. 1. Myo5p co-immunoprecipitates with Cmd1p. (**A**) Specificity control for Cmd1p (α-Cmd1p) and myc-tagged Myo5p (α-myc) detection. For Cmd1p detection, total protein extracts from the wt strain RH3975 (CMD1, EGTA, Ca^{2+}) or from the *cmd1-228* mutant (strain RH3985) were separated on a 15% SDS–polyacrylamide gel and processed for immunoblotting using the α-Cmd1p polyclonal serum raised against purified recombinant Cmd1p. 100 mM EGTA or $CaCl_2$ was added to the EGTA and Ca^{2+} samples, respectively. For myc-tagged Myo5p detection, protein extracts from *myo5*Δ strains (strain RH3976) bearing either pA12myc*MYO5* (myc*MYO5*) or pA12*MYO5* (*MYO5*) were separated on a 7.5% SDS–polyacrylamide gel and processed for immunoblot using the α-myc 9E10 monoclonal antibody. (**B**) Co-immunoprecipitation experiments. *myo5*Δ (strain RH3976) strains bearing pA12myc*MYO5* (EGTA, Ca2+, preimmune) or pA12*MYO5* (no myc) were grown to log-phase, harvested, lysed using glass beads and a high speed pellet was prepared. Myo5p was solubilized in a high salt buffer containing 5 mM ATP and 1 mM EGTA. The extracts were immunoprecipitated using the α-Cmd1p antibody (EGTA, Ca^{2+}, no myc) or a preimmune serum (preim.). $CaCl_2$ (5 mM) was added to the Ca^{2+} sample. The immunoprecipitates (P) and supernatants (S) were processed for Cmd1p and myc-tagged Myo5p detection by immunoblotting using the α-Cmd1p or the α-myc antibodies.

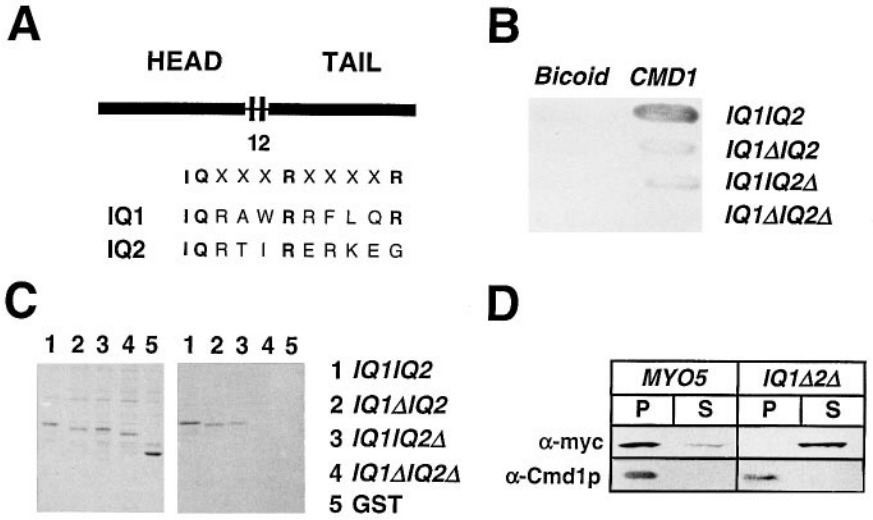

Fig. 2. Myo5p binds Cmd1p through the IQ motifs located at the neck. (**A**) Sequence of the Myo5p peptides that fit the IQ consensus and schematic representation of their locations in the protein. (**B**) Two-hybrid detection of the IQ1-, IQ2-motif–Cmd1p interaction. The Myo5p neck region containing IQ1 and IQ2 (IQ1IQ2) or the same region where IQ1 (IQ1ΔIQ2), IQ2 (IQ1IQ2Δ), both (IQ1ΔIQ2Δ) were deleted, were cloned after the B42 transcriptional activator acid loop (pJG4-5 series). *CMD1* was fused to the lexA DNA binding domain of pEG202 (pEG202*CMD1*). The constructs were transformed into EGY48 bearing the β-galactosidase reporter gene downstream of eight lexA binding sites (pSH18-34). Enzyme activity caused by interaction between the lexA and B42 fused proteins was monitored on X-Gal-containing plates. As a specificity control the bicoid protein from *Drosophila melanogaster* (BICOID) fused to B42 was also used as prey. (**C**) Overlay assay detection of the IQ1-, IQ2-motif–Cmd1p interaction. The same *MYO5* sequences as described in B were fused to GST and expressed in *E.coli*. Total bacterial protein extracts were separated using 15% polyacrylamide gels and either stained with Coomassie Blue (left panel), or processed for the overlay assay (right panel). In the latter, proteins were transferred to a nitrocellulose filter, partially renatured, and incubated with ^{35}S-labeled purified recombinant Cmd1p. After washing, the filters were dried and exposed to an X-ray film. (**D**) Deletion of IQ1 and IQ2 disrupts Cmd1p–Myo5p interaction in a co-immunoprecipitation experiment. *myo5*Δ (strain RH3976) strains bearing pA12myc*MYO5* (*MYO5*) or pA12myc*myo5-IQ1*Δ*2*Δ (*IQ1*Δ*2*Δ) were grown to log-phase, harvested, lysed using glass beads and a high speed pellet was prepared. Myo5p was solubilized in a high salt buffer containing 5 mM ATP and 1 mM EGTA. Extracts were immunoprecipitated with the α-Cmd1p antibody. Immunoprecipitates (P) and supernatants (S) were processed for detection of Cmd1p or the myc-tagged wt or mutant Myo5p by immunoblotting using the α-Cmd1p or α-myc antibodies.

The immunoprecipitates (P) and the supernatants (S) were then analyzed for Cmd1p or Myo5p content by immunoblot using the α-Cmd1p and the 9E10 antibodies, respectively (Figure 1B, EGTA). Myo5p was recovered in the Cmd1p immunoprecipitates under these conditions. The same results were obtained using α-Cmd1p serum or affinity purified α-Cmd1p IgG from another source [kindly provided by T.Davis, U.Washington, Seattle (data not shown)]. As controls, the same experiment was performed using a preimmune serum (Figure 1B., preim.) or a strain expressing the non-tagged version of Myo5p (Figure 1B, no myc). Similar to findings with other type I myosins, the Cmd1p–Myo5p interaction was disrupted with 5 mM $CaCl_2$ in the immunoprecipitation buffer (Figure 1B, Ca^{2+}).

The IQ motifs in the neck region of Myo5p are necessary and sufficient for Cmd1p binding

Two IQ motifs are present at the Myo5p neck (IQ1 and IQ2) whose sequence and location in the protein is schematically represented in Figure 2A. In order to analyze whether any of these sequences could mediate binding to Cmd1p, we first used the two-hybrid system. We fused the neck region of Myo5p including the IQ motifs flanked by 20 amino acids N- and C-terminally, after the B42 transcriptional activator domain. *CMD1* was fused to the lexA DNA binding domain. The constructs were transformed into EGY48 bearing the β-galactosidase reporter gene downstream of 8 LexA binding sites (pSH18–34) and interaction was monitored on X-Gal-containing plates (Figure 2B). A strong β-galactosidase activity was detected in the strain bearing the LexA–Cmd1p (*CMD1*) fusion and the B42-Myo5p neck region (IQ1IQ2) fusion protein. Deletion of either IQ1 (IQ1ΔIQ2) or IQ2 (IQ1IQ2Δ) diminished, but did not abolish, interaction. Only deletion of both IQ motifs (IQ1ΔIQ2Δ) completely abrogated the interaction in this assay. As a control, LexA fused to the *Drosophila melanogaster* protein, bicoid, was used instead of the *CMD1* fusion and it showed no interaction.

In order to confirm the specificity of the interaction between the Myo5p neck region and Cmd1p, we searched the yeast genome data bank for genes that encode proteins less than 200 amino acids in length with homology to calmodulin. Six were identified (DDBJ/EMBL/GenBank accession numbers M14078, Z72628, X69765, X74151, U25841 and U28373). Each gene was fused in-frame to the lexA binding domain coding sequence of pEG202. None of them interacted with the IQ1IQ2-B42 prey construct, showing no detectable development of blue color (data not shown).

In order to confirm the two-hybrid results and to determine whether the interaction between Cmd1p and the Myo5p IQ motifs was direct, an overlay assay was performed. The same IQ constructs as for the two-hybrid experiments were fused to the C-terminus of GST and expressed in *Escherichia coli*. Total bacterial protein extracts were separated by SDS–PAGE and either stained with Coomassie Blue (Figure 2C, left panel) or processed for the Cmd1p overlay assay (Figure 2C, right panel). In the latter case, proteins were transferred to a nitrocellulose filter, renatured, incubated in the presence of ^{35}S-labeled

purified recombinant Cmd1p, dried and exposed to X-ray film. Consistent with the two-hybrid results, maximal binding to Cmd1p was observed for the IQ1IQ2 fusion protein (lane 1) and deletion of either IQ1 (lane 2) or IQ2 (lane 3) diminished, but did not abolish, interaction. No interaction was detected for any of the other constructs. These results indicated that the interaction between the Myo5p neck region and Cmd1p is direct.

In order to determine whether the IQ motifs are necessary for Cmd1p–Myo5p interaction in the context of the whole Myo5p molecule, a myc-tagged *myo5* mutant was generated where the IQ motifs were deleted (*myo5-IQ1Δ2Δ*). This allele was subcloned into a 2μ plasmid and used for a co-immunoprecipitation experiment with the α-Cmd1p antibody as described above. Deletion of the IQ motifs completely abrogated Cmd1p–Myo5p interaction in this assay (Figure 2D).

Deletion of the calmodulin binding sites in Myo5p only partially impairs its endocytic function

In order to determine whether Cmd1p binding is required for Myo5p function, we substituted the mutant *myo5-IQ1Δ2Δ* for the wt *MYO5* in the yeast genome. This strain was then crossed to a *myo3*Δ strain in order to generate the *myo3*Δ*myo5-IQ1Δ2Δ* double mutant. A representative tetrad dissection from the *myo3Δ/MYO3 myo5-IQ1Δ2Δ/MYO5* diploid is shown in Figure 3A. As controls, *myo3Δ/MYO3 myo5Δ/MYO5* and *myo3Δ/MYO3 MYO5/MYO5* strains were also dissected. As previously described, the predicted *myo3*Δ *myo5*Δ double mutant spores (*myo3Δ/MYO3 myo5Δ/MYO5*, filled circles) failed to grow in our strain background (Geli and Riezman, 1996). In contrast, *myo3*Δ *myo5-IQ1Δ2Δ* (*myo3Δ/MYO3 myo5-IQ1Δ2Δ/MYO5*, filled circles) showed wt viability and growth at 24°C, suggesting that Myo5-IQ1Δ2Δp was at least partially functional at this temperature. In order to determine whether the Myo5-IQ1Δ2Δp was functional for endocytosis, we assayed a *myo3*Δ *myo5-IQ1Δ2Δ* strain for α-factor uptake (Figure 3B, *myo5-IQ1Δ2Δ*) and compared it with a *myo3*Δ *MYO5* strain that shows wt internalization kinetics (Figure 3B, *MYO5*). Myo5-IQ1Δ2Δp was able to drive α-factor internalization in a *myo3*Δ mutant with a rate close to wt at 24°C. However, we observed that α-factor uptake and growth were impaired at higher temperatures. Uptake was completely blocked at 37°C (Figure 3B) and the inactivation was not reversible, suggesting that this protein might unfold at high temperatures. Mutant Myo5p proteins where only IQ1 or IQ2 were deleted sustained α-factor uptake kinetics with nearly wt kinetics, both at 24°C or 37°C (data not shown).

Cmd1p fulfills at least two distinct functions in the uptake step of receptor-mediated endocytosis in yeast

The data depicted above could indicate that Cmd1p binding to Myo5p is dispensable for the endocytic function and may suggest a role for Cmd1p as a negative regulator of myosin function. However, it could also be possible that Cmd1p binding to Myo5p is required to block an autoinhibitory domain of Myo5p which overlaps with the IQ motifs. In fact, the calmodulin binding sites of many calmodulin-activated enzymes have been mapped to amphiphylic α-helices that function as autoinhibitory domains (James *et al*., 1995). In this case, disruption of the Cmd1p–Myo5p interaction would only have an inhibitory effect on the uptake assay in the presence of the intact Myo5p, but not in the *myo5-IQ1Δ2Δ* strain.

In order to differentiate between these two hypotheses, we decided to disrupt the interaction between Cmd1p and wt Myo5p using *cmd1* mutant alleles and to analyze these mutants in terms of their endocytic phenotype. Since calmodulin is a multifunctional protein, *cmd1* alleles impaired in binding to distinct targets would greatly facilitate this approach. For that purpose, we decided to analyze the ts *cmd1* mutant collection described by Ohya and Botstein (1994a, b). The ts recessive alleles generated by these authors can be classified into four intragenic complementation groups (A, B, C and D), each bearing distinct, major phenotypic defects: actin cytoskeleton disorganization, calmodulin delocalization, nuclear division and budding defects, respectively. These findings suggest that calmodulin fulfills at least four different essential functions in the yeast cell, which are specifically impaired in mutants belonging to the different intragenic complementation groups.

We assayed the different ts *cmd1* alleles for their ability to internalize α-factor at the restrictive temperature (37°C). The results are summarized in Figure 4A. Cells were considered negative for endocytosis (–) if the α-factor uptake rates were less than 15% of the wt at 37°C. Cells were considered positive (+) if they showed nearly wt uptake kinetics. We observed that mutants from intragenic complementation groups A and B were negative for α-factor uptake at the restrictive temperature, whereas mutants from intragenic complementation groups C and D showed wt uptake kinetics. Consistent with this, alleles that could not complement mutants in groups B, C and D were also defective for α-factor uptake. We also found that one *cmd1* allele, originally classified as partially dominant (*cmd1-247*) (Ohya and Botstein, 1994b), was defective in receptor-mediated internalization at the restrictive temperature.

The data presented above suggest that at least two distinct calmodulin functions are required for the uptake step of receptor-mediated endocytosis in yeast. Since the growth and endocytic defects are not necessarily caused by disruption of binding to the same Cmd1p target for a given *cmd1* mutant, we redefined the intragenic complementation groups for the defective mutants (*cmd1-226*, *cmd1-228*, *cmd1-247*) in terms of their endocytic phenotype. For that purpose, we transformed the *CMD1*, *cmd1-226*, *cmd1-228* and *cmd1-247* strains with centromeric plasmids bearing the different alleles (p*CMD1*, p*cmd1-226*, p*cmd1-228* and p*cmd1-247*) and assayed them for α-factor internalization at 37°C. The results, expressed as percentage of bound α-factor internalized per min in the linear range, are shown in Figure 4B. The results indicate that all the *cmd1* mutants analyzed behave as recessive alleles in terms of their endocytic phenotype (including *cmd1-247*) because expression of wt Cmd1p completely restored uptake. This suggests that these mutations impair calmodulin function because it can no longer interact with the different targets. Furthermore, expression of Cmd1-228p and Cmd1-247p in the same cell restored α-factor internalization kinetics to wt levels suggesting that these two alleles affect two distinct functions, both required for

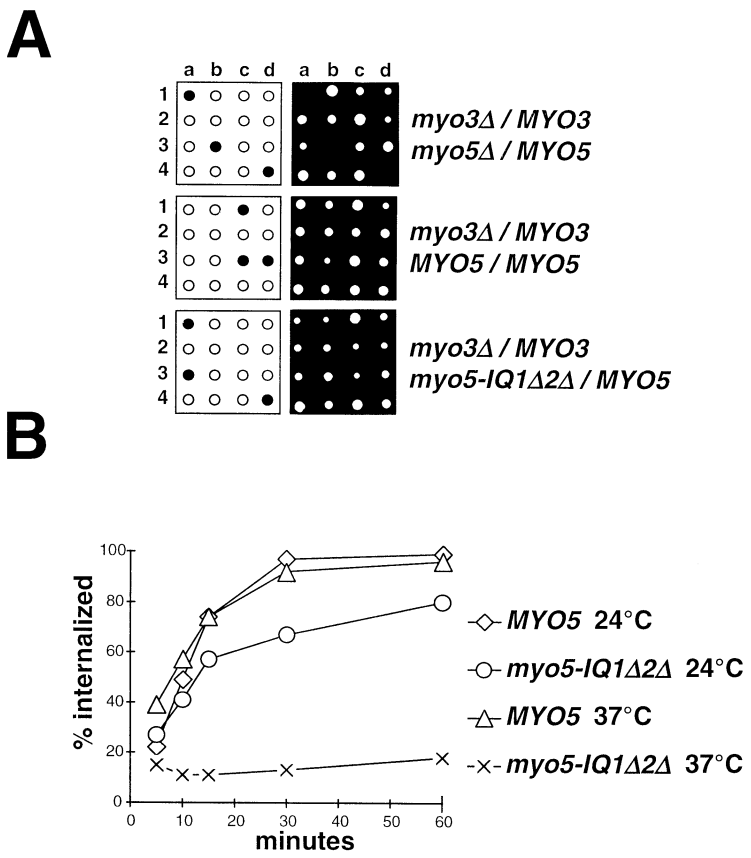

Fig. 3. A mutant Myo5p lacking IQ1 and IQ2 (Myo5-IQ1Δ2Δp) is partially active. (**A**) *myo3Δmyo5-IQ1Δ2Δ* spores are viable. *MYO5* or the mutant *myo5-IQ1Δ2Δ* alleles were integrated at the *MYO5* locus in a *myo5Δ* strain (strain RH3978) and crossed to a *myo3Δ* strain (strain RH3977) to generate strains RH4013 and RH4014, respectively. Strains RH3375 (*myo3Δ/MYO3 myo5Δ/MYO5*), RH4013 (*myo3Δ/MYO3 MYO5/MYO5*) and RH4014 (*myo3Δ/MYO3 myo5-IQ1Δ2Δ/MYO5*) were sporulated and dissected. Filled circles indicate either predicted double mutants (for RH3375 or RH4014) or *myo3Δ MYO5* spores (for RH4013) where the *MYO5* allele is the integrated copy. (**B**) Myo5-IQ1Δ2Δp can partially sustain α-factor uptake in a *myo3Δmyo5Δ* background. A *MAT***a** *myo3Δ myo5-IQ1Δ2Δ* (strain RH3982, *myo5-IQ1Δ2Δ*) strain was assayed for its ability to internalize α-factor and compared with a *myo3Δ MYO5* strain (strain RH3979, *MYO5*) that showed wt kinetics. Cells were grown to 0.5–1×10^7 cells/ml, harvested and incubated in YPUATD on ice for 45 min in the presence of ^{35}S-labeled α-factor. Internalization was triggered by resuspending the cells in 24°C or 37°C YPUATD. Samples were taken at the indicated time points. The percentage of total bound c.p.m. (pH 6 resistant) that were internalized (pH 1 resistant) are indicated. Values correspond to the mean of at least two independent experiments. Standard deviations were <15% of each value.

endocytosis. In contrast, the *cmd1-226* allele was only partially complemented by *cmd1-228* or *cmd1-247*, suggesting that this allele might affect both functions. We also observed that an extra copy of *cmd1-247* partially restored endocytosis, suggesting that this mutant allele might be slightly weaker than *cmd1-226* and *cmd1-228* in terms of its endocytic defect. A partial suppression of the growth defect by expression of an extra copy of a *cmd1* mutant allele has been described previously (Ohya and Botstein, 1994b).

Myo5p might be one of the Cmd1p targets for endocytosis

In order to analyze whether any of the *cmd1* defective alleles were specifically affected in Myo5p function, we examined the effect of overexpressing *MYO5* in the different *cmd1* strains. If any of the *cmd1* mutations resulted in a weakened interaction to Myo5p, the cause of the endocytic defect, overexpression of the target protein might restore α-factor uptake by increasing the amount of Myo5p–Cmd1p active complex per cell. We introduced a 2μ plasmid bearing *MYO5* (p195myc*MYO5*) in the *CMD1*, *cmd1-226*, *cmd1-228* and *cmd1-247* strains. Overexpression of Myo5p in each strain was monitored by immunoblot using the EW and IK antibodies raised against peptides of the Myo5p tail (Figure 5, lower panel). Overexpression of Myo5p specifically restored α-factor internalization in the *cmd1-247* mutant (Figure 5, upper panel) at the restrictive temperature (37°C).

The genetic interactions described above suggest the model depicted in Figure 5B for Cmd1p function in endocytosis. According to this model, Cmd1p interacts with two different targets that are both required for the uptake step of receptor-mediated endocytosis in yeast. Myo5p would be one of the targets. Cmd1p–Myo5p interaction would specifically be impaired in the *cmd1-247* mutant, whereas the *cmd1-228* mutation would affect binding to the other endocytic target. The *cmd1-226* mutant allele would be affected in binding to both targets.

In order to test some of the predictions of this hypothesis, we examined the ability of the proteins encoded by the different *cmd1* alleles to interact with Myo5p, using the two-hybrid system. The *cmd1* mutant alleles belonging to complementation groups A, B, C or D were cloned after the lexA DNA binding domain coding sequence of pEG202 to assess their ability to interact with the neck region of

A

GROUP	MUTANT	UPTAKE
A	*cmd1-226*	–
B	*cmd1-228*	–
C	*cmd1-239*	+
	cmd1-250	+
D	*cmd1-231*	+
	cmd1-233	+
B C D	*cmd1-234*	–
	cmd1-235	–
	cmd1-251	–
DOMINANT	*cmd1-242*	+
	cmd1-247	–

B

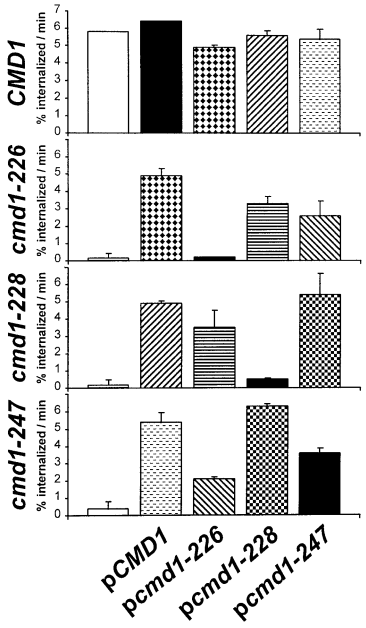

Fig. 4. At least two distinct Cmd1p functions are required in the uptake step of receptor-mediated endocytosis. (**A**) Analysis of the endocytic phenotype of the ts *cmd1* mutant collection. *cmd1* ts mutants classified into intragenic complementation groups A (strain RH3984), B (strain RH3985), C (strain RH3988 and RH3989), D (strain RH33986 and RH3987) or B, C and D (strains RH4015, RH4016 and RH4017) or those classified as partially dominant (DOMINANT) (strain RH3990 and RH3991) (Ohya and Botstein, 1994a, b) were grown to 0.5–1×10^7 cells/ml, harvested and resuspended in 37°C YPUATD. After 10 min preincubation, ^{35}S-labeled α-factor was added and samples were taken at 5, 10 and 15 min after addition of α-factor. (–) indicates uptake rates (percentage of c.p.m. internalized per min.) <15% of the wt rate. (+) indicates wt uptake kinetics. (**B**) Complementation analysis of the endocytic defect of *cmd1-226*, *cmd1-228* and *cmd1-247* mutants. *CMD1* (strain RH3983), *cmd1-226* (strain RH3984), *cmd1-228* (strain RH3985) and *cmd1-247* (strain RH3991) were transformed with the pRS416-derived centromeric plasmids bearing the different alleles (p*CMD1*, p*cmd1-226*, p*cmd1-228*, p*cmd1-247*). The cells were grown on SDYE-URA for plasmid selection and α-factor internalization monitored at 37°C as described above. The bars indicate percentage of α-factor counts internalized per min. Empty bars correspond to the strains bearing no plasmid. Black bars correspond to strains bearing the plasmid with the same allele as the genomic copy. Bars with identical patterns correspond to uptakes of cells expressing the same pair of alleles but with reciprocal genomic versus plasmid locations.

Myo5p. β-galactosidase activity was monitored on X-Gal containing plates as described above. As shown in Figure 6A, we observed that both *cmd1-226* and *cmd1-247* mutant proteins were strongly impaired in binding to the Myo5p neck region (IQ1IQ2) in agreement with the proposed model. All other *cmd1* mutants, including *cmd1-228*, strongly activated transcription of the reporter gene. For some of the alleles (*cmd1-228*, *cmd1-239* and *cmd1-250*), the specificity of the interaction could not be assessed on X-Gal-containing plates because they induced transcription of the reporter gene in the control strains bearing the Myo5p neck region where the IQ motifs were deleted (IQ1ΔIQ2Δ). Nevertheless, when liquid assays for β-galactosidase activity were performed on these strains, a significantly higher activity was detected in the strains bearing the IQ motifs (data not shown).

To confirm the differential behavior of Cmd1-226p and Cmd1-247p versus Cmd1-228p in terms of their ability to bind Myo5p, co-immunoprecipitation experiments using α-Cmd1p antibodies were performed. The different strains were transformed with a 2μ plasmid bearing the myc-tagged *MYO5* (p195myc*MYO5*) and processed as described before. The results are shown in Figure 6B. As suggested by the two-hybrid experiments, Cmd1-226p and Cmd1-247p were impaired in Myo5p binding whereas the Myo5p–Cmd1-228p interaction was comparable with wt (Figure 6B).

Discussion

Myo5p interacts with Cmd1p through two IQ motifs in the Myo5p neck

The experiments presented above indicate that calmodulin and the unconventional myosin Myo5p interact *in vivo* and localize the Cmd1p binding site of Myo5p to the neck of this protein that includes two IQ motifs. The primary evidence that demonstrates the Cmd1p–Myo5p interaction is their co-immunoprecipitation from non-denatured extracts. The specificity of this interaction is strongly supported by the fact that co-immunoprecipitation was abrogated by defined mutations in either Myo5p or Cmd1p (*myo5-IQ1Δ2Δ* or *cmd1-247* and *cmd1-226*). The essential role that both proteins play in the uptake step of receptor-mediated endocytosis and the suppression of the *cmd1-247* endocytic defect by overexpression of *MYO5* strongly suggest that this interaction occurs *in vivo* and is relevant to endocytosis.

The two-hybrid results, the overlay assay and the co-immunoprecipitation experiments define the Myo5p neck as sufficient, and the IQ motifs as necessary, for Cmd1p binding. Furthermore, the overlay assay shows that this interaction is direct. Both IQ motifs seem to contribute to this interaction since deletion of either one diminished, but did not abolish binding in the two-hybrid and the overlay assays. Using these techniques, we cannot deter-

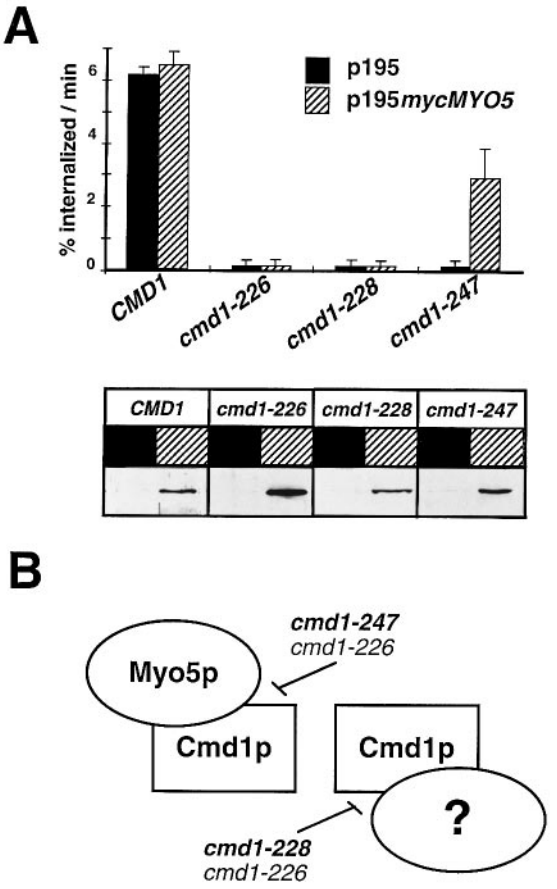

Fig. 5. Overexpression of Myo5p specifically suppresses the uptake defect of *cmd1-247*. (**A**) *CMD1* (strain RH3983), *cmd1-226* (strain RH3984), *cmd1-228* (strain RH3985) and *cmd1-247* (strain RH3991) cells, were transformed with a 2μ plasmid bearing *MYO5* (p195myc*MYO5*) (p195*MYO5*) or the empty plasmid (YEplac195) (p195) and the strains were assayed for α-factor uptake at the restrictive temperature (37°C) as described in Figure 4. The lower panel corresponds to the immunoblot analysis of the indicated strains using the EW and IK antibodies. (**B**) Model for Cmd1p endocytic function suggested by the genetic interactions. The *cmd1-228* and *cmd1-247* mutations would disrupt interaction with two different target proteins. Binding between Cmd1p and each of these targets would be required for the uptake step of receptor-mediated endocytosis in yeast. The target whose interaction with Cmd1p would be disrupted in the *cmd1-247* mutant would be the unconventional type I myosin Myo5p. The *cmd1-226* mutation would most likely affect binding to both targets.

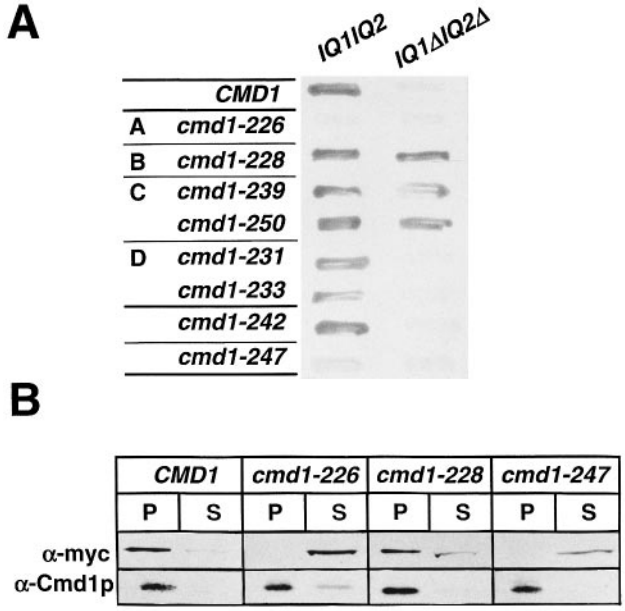

Fig. 6. Cmd1p–Myo5p interaction is weakened by the *cmd1-226* and the *cmd1-247* mutations. (**A**) Two-hybrid analysis of the interaction between *cmd1* alleles and the Myo5p neck. The indicated *cmd1* alleles fused to the lexA DNA-binding domain of pEG202 were transformed into EGY48 bearing the β-galactosidase reporter gene (pSH18-34) and the Myo5p neck (pJG4-5*IQ1IQ2*) (IQ1IQ2) or the same sequence with the IQ motifs deleted (pJG4-5*IQ1ΔIQ2Δ*) (IQ1ΔIQ2Δ) as control fused to the B42 transcriptional activator loop of pJG4-5. β-galactosidase activity was monitored on X-Gal plates as described in Figure 2B. (**B**) *cmd1-226* and *cmd1-247* mutations impair Myo5p–Cmd1p interaction in a co-immunoprecipitation experiment. *CMD1* (strain RH3976) bearing pA12myc*MYO5* or the *cmd1-226* (strain RH3984), *cmd1-228* (strain RH3985) and *cmd1-247* (strain RH3991) mutants bearing p195myc*MYO5* were grown to log-phase, harvested, lysed using glass-beads and a high speed pellet was prepared. myc-tagged Myo5p was solubilized in a high salt buffer containing 5 mM ATP and 1 mM EGTA. The extracts were immunoprecipitated using the α-Cmd1p antibody. The immunoprecipitates (P) and supernatants (S) were processed for immunoblot detection of Cmd1p and myc-tagged Myo5p using α-Cmd1p and α-myc antibodies, respectively.

mine whether the diminished binding was caused by a decreased overall affinity or a lower number of Cmd1p binding sites. The specificity of the Myo5p neck–Cmd1p interaction observed in the two-hybrid experiments is strongly supported by the fact that it is disrupted in the same *cmd1* mutants that impair Cmd1p–Myo5p interaction in the co-immunoprecipitation experiments (*cmd1-247*, *cmd1-226*). Deletion of the IQ motifs of Myo5p also abolishes interaction with Cmd1p in a co-immunoprecipitation experiment. This result suggests that the Myo5p neck is the major, if not the only Cmd1p binding site in Myo5p.

The yeast *MYO5* and *MYO3* show highest homology to the protozoal type I myosins (Goodson and Spudich, 1995; Geli and Riezman, 1996; Goodson *et al*., 1996). These myosins do not seem to interact with calmodulin but rather with other small members of the EF-hand-containing protein family (Maruta *et al*., 1978). This does not seem to be the case for Myo5p. A Cmd1p–Myo5p interaction was demonstrated using different techniques, whereas six different calmodulin-related proteins failed to interact with the Myo5p neck in the two-hybrid system. In this respect, the yeast type I myosins may resemble the vertebrate members of the group. Strikingly, the rat myosin I myr 3, which is also closely related to the protozoal type I myosins, has also been shown to use calmodulin as the light-chain (Wang *et al*., 1997).

Myo5p–Cmd1p interaction is most likely required to support receptor-mediated internalization in vivo

To date, the requirement of calmodulin for type I myosin function has never been demonstrated *in vivo*. This subject has mainly been addressed *in vitro* and the results obtained seem to be quite variable. Ca^{2+}-dependent disruption of myosin–calmodulin interaction resulted in inhibition of an actin sliding assay using the avian Brush Border Myosin I (BBMI) and, therefore, a positive requirement of calmodulin for myosin function was suggested. However, Ca^{2+}-dependent calmodulin release from the same myosin strongly activated its Mg^{2+}-ATPase indicating a putative

role of calmodulin as a negative myosin regulator (Collins *et al*., 1990; Wolenski *et al*., 1993). The data presented in this article strongly suggest that the Cmd1p–Myo5p interaction is essential for endocytosis. The fact that Cmd1p and Myo5p directly interact and that both proteins are required in the endocytic process already suggested this. However, more direct evidence comes from the study of the *cmd1-247* mutant. The *cmd1-247* mutation caused a recessive ts endocytic defect, as judged by the complementation experiments, suggesting that it impaired this process because Cmd1-247p could no longer interact with its relevant target for endocytosis. Consistent with these findings, we showed by two-hybrid and co-immunoprecipitation experiments that this mutation specifically weakened binding to Myo5p compared with the wt *CMD1* or to other *cmd1* mutations that are permissive for endocytic uptake. Additionally, overexpression of Myo5p specifically suppressed the endocytic defect of the *cmd1-247* mutant, further indicating that Myo5p is the relevant Cmd1p target whose endocytic function is impaired in the *cmd1-247* mutant and that this endocytic defect is caused by a lack of interaction between the two proteins. It should be mentioned that both the two-hybrid and the co-immunoprecipitation experiments revealed a weakened interaction between the Cmd1-226 and Cmd1-247 mutant proteins and Myo5p already at permissive temperature, suggesting that this type of analysis *in vitro* is more stringent than the conditions *in vivo* where a more short-lived interaction could suffice.

Since the Cmd1p–Myo5p interaction is required for endocytosis, it may appear surprising that deletion of the calmodulin binding site of Myo5p (*myo5-IQ1Δ2Δ*) does not seem to have a major effect on myosin function at 24°C. Myo5-IQ1Δ2Δp is at least partially functional for growth and endocytosis in a *myo3Δmyo5-IQ1Δ2Δ* strain. A satisfactory explanation of this apparent discrepancy would be that the calmodulin binding sites overlap with an auto-inhibitory domain of Myo5p and that Cmd1p serves to counteract this inhibition. Indeed, many calmodulin-activated enzymes possess autoinhibitory domains that overlap with their calmodulin binding sites (James *et al*., 1995). Removal of the calmodulin binding sites from the cAMP phosphodiesterase (Klee *et al*., 1980), the plasma membrane Ca^{2+}-pump ATPase (Zurini *et al*., 1984), the myosin light-chain kinase (Edelman *et al*., 1985) or the cysteine protease calpain (James *et al*., 1989) produced constitutively active enzymes, similar to what we observed for Myo5p *in vivo*. In addition, BBMI head fragments, where the IQ motifs have been proteolytically removed, showed elevated Mg^{2+}-ATPase activity, suggesting that the presence of an auto-inhibitory domain, which overlaps with the IQ motifs, may be a general feature of the type I myosins (Wolenski *et al*., 1993).

In addition, our results are in striking agreement with what has been described for the conventional myosin II regulatory light-chains (RLC). Removal of the RLC from the scallop myosin II using EDTA results in reduced ATPase and actin motility activity *in vitro* (Vale *et al*., 1984). In agreement, reduced amounts of RLC transcript in *D.melanogaster* produce phenotypes clearly associated to myosin II misfunction (Karess *et al*., 1991; Warmke *et al*., 1992). In contrast, removal of the RLC binding site of the *Dictyostelium* myosin II renders a functional protein that is able to complement a strain deleted for the chromosomal myosin II gene and that shows even higher ATPase activity than the wt protein *in vitro* (Uyeda and Spudich, 1993).

The Myo5-IQ1Δ2Δp does not seem to be functional at high temperatures. A *myo3Δ myo5-IQ1Δ2Δ* strain showed impaired growth at 37°C and was completely blocked for α-factor uptake at this temperature. Two possible explanations for this can be proposed. First, calmodulin binding to Myo5p may only be required at elevated temperatures, even in the absence of the IQ motifs. Second, and perhaps more likely, the mutant protein may simply misfold or denature at high temperatures as a consequence of the deletion of the IQ region. Consistent with the latter explanation, Myo5-IQ1Δ2Δp inactivation at 37°C was not reversible. On the other hand, the endocytic defect in the *cmd1-247* mutant was fully reversible when cells were shifted back to permissive temperature, indicating that the cause of its endocytic defect at 37°C is different from that of the *myo3Δ myo5-IQ1Δ2Δ* mutant.

Cmd1p fulfills an additional function required in the uptake-step of receptor-mediated endocytosis

The intragenic complementation of the *cmd1-247* and *cmd1-228* mutants in terms of their endocytic defect strongly indicates that Cmd1p fulfills at least two different functions, both required for the uptake step of receptor-mediated endocytosis in yeast. Expression of Cmd1-228p and Cmd1-247p proteins in the same cell restored α-factor uptake to wt levels, whereas strains expressing either mutant protein alone were completely blocked for receptor-mediated endocytosis at the restrictive temperature. This finding was not due to a dosage effect because it was allele specific and it was observed whether the *cmd1-228* or the *cmd1-247* allele were located on a centromeric plasmid or in the genome. The fact that both mutations are recessive for their endocytic phenotype, indicates that they most likely impair Cmd1p function by preventing Cmd1p binding to independent targets. Cmd1p–Myo5p binding seems to be much stronger in the *cmd1-228* than in the *cmd1-247* mutant as assessed by the two-hybrid and co-immunoprecipitation experiments, indicating that Myo5p is not the relevant Cmd1p target whose function is affected in *cmd1-228*. Consistent with this proposal, Myo5p overexpression did not rescue the *cmd1-228* endocytic defect.

Is Myo5p function regulated in a Ca^{2+}-dependent manner?

Data obtained *in vitro* with many different type I myosins suggest that calmodulin confers Ca^{2+} sensitivity to myosin regulation (Wolenski, 1995). For instance, the avian BBMI copurified with four calmodulin molecules in the presence of EGTA. Addition of Ca^{2+} caused partial dissociation of calmodulin, concomitant with progressive inhibition of motility in an actin sliding assay (Collins *et al*., 1991; Wolenski *et al*., 1993). When the calmodulin binding sites of BBMI were proteolytically removed, the resulting head fragment showed elevated Mg^{2+}-ATPase activity, which was then completely insensitive to Ca^{2+} (Wolenski *et al*., 1993).

We observed that addition of $CaCl_2$ disrupted Cmd1p–Myo5p interaction in a co-immunoprecipitation experi-

ment, suggesting that a Ca^{2+}-dependent regulation of Myo5p is potentially possible. However, whether Cmd1p–Myo5p dissociation occurs in response to micromolar variations in the intracellular Ca^{2+} concentrations and whether a tight Ca^{2+}-regulated switch between activated and inactivated Myo5p states is essential to its function *in vivo* is still an open question. In fact, a Ca^{2+}-independent Cmd1p-binding requirement for Myo5p function in endocytosis is consistent with the endocytic phenotype of the *cmd1-3* mutant allele. This mutant allele bears point mutations in the EF-hand motifs that strongly impairs its ability to bind Ca^{2+} *in vitro* and causes a ts phenotype *in vivo* (Geiser *et al*., 1991). Nevertheless, this mutant is able to support receptor-mediated endocytosis at wt rates (Kübler *et al*., 1994). Consistent with this, we observed that the Cmd1-3p is able to bind Myo5p in the two-hybrid system (data not shown). Unfortunately, our α-Cmd1p antibody does not recognize the Cmd1-3p mutant protein and therefore co-immunoprecipitation experiments to assess its Ca^{2+}-insensitivity with respect to Myo5p binding were not possible. If the Cmd1-3p is truly insensitive to Ca^{2+} regulation *in vivo*, this would indicate that a tight Ca^{2+}-dependent modulation of Myo5p–Cmd1p interaction is not essential for its endocytic function. This view is supported by the fact that Myo5-IQ1Δ2Δp can still sustain endocytosis, albeit less efficiently.

Nevertheless, a Ca^{2+}-dependent regulation of Myo5p could still be essential in other cellular processes where this protein might be involved (Geli and Riezman, 1996; Goodson *et al*., 1996). Additional experiments will be necessary to investigate the role of calcium in endocytosis and whether or not a tight calcium-dependent regulation of the active and the inactive states of Myo5p is required for its function *in vivo*.

In summary, the data depicted above show that Myo5p and Cmd1p physically interact *in vivo* and that this interaction is required for receptor-mediated endocytic internalization in yeast. The results are consistent with a role of Cmd1p as a Myo5p light-chain and suggest that Cmd1p functions by counteracting a Myo5p autoinhibitory domain. Furthermore, the results indicate that Cmd1p fulfills an additional function in the uptake step of receptor-mediated endocytosis. Current isolation and characterization of suppressors of the *cmd1-228* endocytic defect may help to identify the second Cmd1p target required in the uptake step of receptor-mediated endocytosis in yeast.

Materials and methods

Yeast media, strains and genetic techniques

All yeast strains used in this report are listed in Table I with their relevant genotypes. Unless otherwise mentioned, strains that did not bear plasmids were grown in complete media YPUATD [2% glucose, 2% peptone, 1% yeast extract, 40 μg/ml uracil (Ura), 40 μg/ml adenine (Ade) and 40 μg/ml tryptophan (Trp), 2% agar for solid media]. Strains bearing plasmids were selected on SD minimal media (Dulic *et al*., 1991) except liquid cultures for co-immunoprecipitation or α-factor uptake assays, which were grown in SDYE (SD, 0.2% yeast extract). Sporulation, tetrad dissection and scoring of genetic markers was performed as described by Sherman *et al.* (1974). Recombinant lyticase was purified from *E.coli* as described in Hicke *et al*. (1997). Transformation of yeast cells was accomplished by the lithium acetate method of Ito *et al.* (1983).

RH3975 to RH3978 were generated from RH3375 by inducing sporulation on minimal media, tetrad dissection and scoring of the adequate markers. RH3979 and RH3982 were generated as follows: RH3978 was transformed with pIN*MYO5* or pIN*myo5-IQ1Δ2Δ* (see below) cut with *Sna*BI at the *MYO5* 5′ untranslated region in order to integrate the wild type (wt) or mutant myosins at the *MYO5* locus. This introduces a *URA3* marker at the *MYO5* locus, which can easily be followed in crosses. At least six different colonies that grew on SD-Ura plates from each transformation were then independently crossed to RH3977 to generate the RH4013 and RH4014 diploids that were selected on SD-Ura-histidine(His)-Trp. Diploids were subsequently sporulated, dissected and the tetrads scored for linkage between the *URA3* and *TRP1* markers to verify integration of *MYO5* or *myo5-IQ1Δ2Δ* at the *MYO5* locus. *MAT***a** *myo3Δ MYO5* or *myo3Δmyo5-IQ1Δ2Δ* segregants from each respective diploid were chosen and analyzed for expression of wt or mutant Myo5p by immunoblot using the EW and IK antibodies (see below). Segregants with similar expression levels were used to perform the uptake assays.

RH3983 to RH3991 and RH4015 to RH4017 were generated from the strains YOC200, YOC226, YOC228, YOC231, YOC233, YOC239, YOC250, YOC242, YOC247, YOC234, YOC235 and YOC251 (Ohya and Botstein, 1994b), respectively, by disrupting the *BAR1* gene at its unique *Sal*I site using a *bar1Δ::LYS2* disruption cassette (Kübler and Riezman, 1993).

DNA techniques and plasmid constructions

All DNA manipulations were performed according to standard techniques (Sambrook *et al*., 1989) unless otherwise specified. Restriction enzymes, Klenow and T4 DNA ligase were obtained from Boehringer Mannheim, New England Biolabs, United States Biochemical or Stratagene Cloning Systems. Plasmids were purified by the Qiagen plasmid purification kit (Qiagen), and transformation of *E.coli* was performed by electroporation (Dower *et al*., 1988). All PCRs for cloning purposes were performed with a DNA polymerase with proof reading activity (Pfu, Stratagene Cloning Systems) and a TRIO-thermoblock (Biometra GmbH). Oligonucleotides were synthesized by Microsynth GmbH. All constructs were sequenced using a United States Biochemical Sequenase II DNA sequencing kit and a sequi-gen DNA sequencing gel from Bio-Rad Laboratoires.

All plasmids used in this report are listed in Table II. *myo5-IQ1Δ* *myo5-IQ2Δ* and *myo5-IQ1Δ2Δ* alleles were generated by two step PCR from *MYO5*, deleting the sequences that encode IQRAWRRFLQR (IQ1), IQRTIRERKEG (IQ2) or both. All alleles were cloned at the *Sal*I site of the centromeric plasmid YCplac33 (Gietz and Sugino, 1988) where the *Eco*RI to *Sma*I sites of the polylinker were previously deleted. Using this procedure, p33*MYO5*, p33*myo5-IQ1Δ*, p33*myo5-IQ2Δ* and p33*myo5-IQ1Δ2Δ* were generated. The myc-tagged versions of *MYO5* and *myo5-IQ1Δ2Δ* were constructed on these plasmids by introducing a sequence encoding EQKLISEEDLN (Evan *et al*., 1985) after the initiation codon (ATG) to create p33myc*MYO5* and p33myc*myo5IQ1Δ2Δ*. The different alleles were subcloned into the *Bam*HI and *Sph*I sites of a 2μ version of YEp24 (Sotz and Linder, 1990), pASZ12 (kindly provided by Prof. P.Philippsen), to generate the pA12 series, or YEplac195 (Gietz and Sugino, 1988) to generate p195myc*MYO5*. pIN*MYO5* and pIN*myo5-IQ1Δ2Δ* (used to integrate the alleles) were generated from p33*MYO5* and p33*myo5-IQ1Δ2Δ* respectively, by deleting the ARS and CEN sequences using the *Nsi*I and *Spe*I sites. The pRS416*CMD1*, pRS416*cmd1-226*, pRS416*cmd1-228*, and pRS416*cmd1-247* were constructed by subcloning the *Cla*I–*Bam*HI fragment of each allele (from the original pRB616 series, Ohya and Botstein, 1994b) into pRS416 (Sikorski and Hieter, 1989). For pEG202-derived plasmids, the different *cmd1* alleles were amplified by PCR from the ATG to the stop codon using the original pRB616 derived plasmids or genomic DNA as templates. Convenient restriction sites (*Bam*HI, *Xho*I) were included in the primers in order to subclone the fragments in frame with the lexA DNA binding domain of pEG202 (Ruden *et al*., 1991). The pJG4-5-derived plasmids were constructed as follows: primers with the appropriate restriction sites at the 5′ and 3′ ends (*Eco*RI and *Xho*I) were used to amplify by PCR the sequence encoding the neck region of Myo5p containing the IQ motifs flanked by 20 amino acids N- and C-terminal (pJG4-5*IQ1IQ2*). The PCR fragments were subcloned in frame after the B42 acid loop of pJG4-5. The same oligonucleotides were used to create pJG4-5*IQ1ΔIQ2*, pJG4-5*IQ1IQ2Δ* and pJG4-5*IQ1ΔIQ2Δ* using p33*myo5-IQ1Δ*, p33*myo5-IQ2Δ* and p33*myo5-IQ1Δ2Δ*, respectively, as templates. The pGEX-2T series' for expression in *E.coli* were constructed using exactly the same procedure, but using *Bam*HI and *Eco*RI restriction sites to subclone the fragments in frame after the gene encoding for the glutathione *S*-transferase (GST) of pGEX-2T (Pharmacia Biotech). pQE11*CMD1* was created by subcloning the *CMD1* gene in frame after

Table I. Yeast strains

Strain	Genotype	Reference
RH3375	*MAT***a***/MAT***a** *ade2/ADE2 his3/his3 myo3Δ::HIS3/MYO3 myo5Δ::TRP1/MYO5 leu2/leu2 lys2/LYS2 trp1/trp1 ura3/ura3 bar1/bar1*	Geli and Riezman (1996)
RH4013	*MAT***a***/MAT***a** *his3/his3 myo3Δ::HIS3/MYO3 MYO5::URA3::myo5Δ::TRP1/MYO5 leu2/leu2 lys2/LYS2 trp1/trp1 ura3/ura3 bar1/bar1*	this study
RH4014	*MAT***a***/MAT***a** *his3/his3 myo3Δ::HIS3/MYO3 myo5-IQ1Δ2Δ::URA3::myo5Δ::TRP1/MYO5 leu2/leu2 lys2/LYS2 trp1/trp1 ura3/ura3 bar1/bar1*	this study
RH3975	*MAT***a** *ade2 his3 leu2 trp1 ura3 bar1*	this study
RH3976	*MAT***a** *ade2 his3 myo5Δ::TRP1 leu2 trp1 ura3 bar1*	this study
RH3977	*MAT***a** *his3 myo3Δ::HIS3 leu2 trp1 ura3 bar1*	this study
RH3978	*MAT***a** *his3 myo5Δ::TRP1 leu2 lys2 trp1 ura3 bar1*	this study
RH3979	*MAT***a** *his3 myo3Δ::HIS3 MYO5::URA3::myo5Δ::TRP1 leu2 lys2 trp1 ura3 bar1*	this study
RH3982	*MAT***a** *his3 myo3Δ::HIS3 myo5-IQ1Δ2Δ::URA3::myo5Δ::TRP1 leu2 lys2 trp1 ura3 bar1*	this study
RH3983	*MAT***a** *ade2 ade3Δ::CMD1::HIS3 cmd1Δ::TRP1 his3 leu2 lys2 trp1 ura3 bar1Δ::LYS2*	this study
RH3984	*MAT***a** *ade2 ade3Δ::cmd1-226::HIS3 cmd1Δ::TRP1 his3 leu2 lys2 trp1 ura3 bar1Δ::LYS2*	this study
RH3985	*MAT***a** *ade2 ade3Δ::cmd1-228::HIS3 cmd1Δ::TRP1 his3 leu2 lys2 trp1 ura3 bar1Δ::LYS2*	this study
RH3986	*MAT***a** *ade2 ade3Δ::cmd1-231::HIS3 cmd1Δ::TRP1 his3 leu2 lys2 trp1 ura3 bar1Δ::LYS2*	this study
RH3987	*MAT***a** *ade2 ade3Δ::cmd1-233::HIS3 cmd1Δ::TRP1 his3 leu2 lys2 trp1 ura3 bar1Δ::LYS2*	this study
RH3988	*MAT***a** *ade2 ade3Δ::cmd1-239::HIS3 cmd1Δ::TRP1 his3 leu2 lys2 trp1 ura3 bar1Δ::LYS2*	this study
RH3989	*MAT***a** *ade2 ade3Δ::cmd1-250::HIS3 cmd1Δ::TRP1 his3 leu2 lys2 trp1 ura3 bar1Δ::LYS2*	this study
RH3990	*MAT***a** *ade2 ade3Δ::cmd1-242::HIS3 cmd1Δ::TRP1 his3 leu2 lys2 trp1 ura3 bar1Δ::LYS2*	this study
RH3991	*MAT***a** *ade2 ade3Δ::cmd1-247::HIS3 cmd1Δ::TRP1 his3 leu2 lys2 trp1 ura3 bar1Δ::LYS2*	this study
RH4015	*MAT***a** *ade2 ade3Δ::cmd1-234::HIS3 cmd1Δ::TRP1 his3 leu2 lys2 trp1 ura3 bar1Δ::LYS2*	this study
RH4016	*MAT***a** *ade2 ade3Δ::cmd1-235::HIS3 cmd1Δ::TRP1 his3 leu2 lys2 trp1 ura3 bar1Δ::LYS2*	this study
RH4017	*MAT***a** *ade2 ade3Δ::cmd1-251::HIS3 cmd1Δ::TRP1 his3 leu2 lys2 trp1 ura3 bar1Δ::LYS2*	this study
EGY48	*MAT***a** *ura3 trp1 his3 leu2::lexAop6-LEU2*	Gyuris *et al.* (1993)

Table II. Plasmids

Plasmid	Yeast Ori	Yeast Marker	Insert	Reference
Yeplac195	2μ	*URA3*	–	Gietz and Sugino (1988)
Ycplac33	CEN	*URA3*	–	Gietz and Sugino (1988)
p195myc*MYO5*	2μ	*URA3*	myc-tagged *MYO5*	this study
pA12*MYO5*	2μ	*ADE2*	*MYO5*	this study
pA12myc*MYO5*	2μ	*ADE2*	myc-tagged *MYO5*	this study
pA12myc*myo5-IQ1Δ2Δ*	2μ	*ADE2*	myc-tagged *myo5-IQ1ΔIQ2Δ*	this study
pIN*MYO5*	–	*URA3*	*MYO5*	this study
pIN*myo5-IQ1Δ2Δ*	–	*URA3*	*myo5-IQ1Δ2Δ*	this study
p416*CMD1*	CEN	*URA3*	*CMD1*	this study
p416*cmd1-226*	CEN	*URA3*	*cmd1-226*	this study
p416*cmd1-228*	CEN	*URA3*	*cmd1-228*	this study
p416*cmd1-247*	CEN	*URA3*	*cmd1-247*	this study
pJG4-5I*Q1IQ2*	2μ	*TRP1*	B42*IQ1IQ2*	this study
pJG4-5*IQ1ΔIQ2*	2μ	*TRP1*	B42*IQ1ΔIQ2*	this study
pJG4-5*IQ1IQ2Δ*	2μ	*TRP1*	B42*IQ1IQ2Δ*	this study
pJG4-5*IQ1ΔIQ2Δ*	2μ	*TRP1*	B42*IQ1ΔIQ2Δ*	this study
pEG202*CMD1*	2μ	*HIS3*	lexA*CMD1*	this study
pEG202*cmd1-226*	2μ	*HIS3*	lexA*cmd1-226*	this study
pEG202*cmd1-228*	2μ	*HIS3*	lexA*cmd1-228*	this study
pEG202*cmd1-231*	2μ	*HIS3*	lexA*cmd1-231*	this study
pEG202*cmd1-233*	2μ	*HIS3*	lexA*cmd1-233*	this study
pEG202*cmd1-239*	2μ	*HIS3*	lexA*cmd1-239*	this study
pEG202*cmd1-250*	2μ	*HIS3*	lexA*cmd1-250*	this study
pEG202*cmd1-242*	2μ	*HIS3*	lexA*cmd1-242*	this study
pEG202*cmd1-247*	2μ	*HIS3*	lexA*cmd1-247*	this study
pSH18-34	2μ	*URA3*	8 lexA Op. lacZ	Gyuris *et al*. (1993)
pRFHM-1	2μ	*HIS3*	lexAbicoid	Gyuris *et al*. (1993)
pGEX-2T	–	–	GST	this study
pGEX-2T*IQ1IQ2*	–	–	GST*IQ1IQ2*	this study

the His_6 tag of pQE11 (Qiagen). *CMD1* was amplified by PCR from genomic DNA and cloned into pQE11 (cut with *Bam*HI, blunt ended with Klenow, and cut with *Hin*dIII) using the *Rsa*I site of *CMD1*, which cuts one codon upstream of the ATG, and an artificially introduced *Hin*dIII site downstream of the stop codon (after partial digestion).

Protein techniques and antibodies

SDS–PAGE for protein separation was performed as described (Laemmli *et al*., 1970) using a Minigel system (Hoefer Scientific Instruments). 15% acrylamide gels were used to separate Cmd1p and the GST-fusion proteins and 7.5% gels to separate Myo5p. High and low range SDS–PAGE molecular weight standards (Bio-Rad Laboratories) were used for determination of apparent molecular weight. Total yeast protein extractions were performed as described (Horvath and Riezman, 1994), except that 3×10^7 cells were collected (at a culture density of 1.5×10^7 cells/ml) and frozen at –20°C and thawed before extraction. Western blotting was also performed as described (Horvath and Riezman, 1994) with the addition of 0.1% (v/v) Nonidet P-40 in the solutions for blocking

and subsequent incubations. Incubation with primary antibodies, 9E10, α-Cmd1p, EW or IK (see below), was followed by incubation with the secondary antibody conjugated to peroxidase. Membranes were developed using an ECL immunoblotting detection reagent kit (Amersham Life Science), exposed to KODAK XAR X-ray films and developed using a Fuji automatic film developer.

The antibody against Cmd1p (α-Cmd1p) was raised in rabbits by injecting purified Cmd1p (see below). Two different antibodies were raised in rabbits against the Myo5p peptides EEANEDEEEDDW (EW) and IPTPPQNRDVPK (IK) synthesized by Neosystem Laboratoire (Strasbourg, France). Myo5p antibody specificity was assessed on immunoblots by comparing *MYO5* and *myo5*Δ extracts. The 9E10 anti-myc antibody was kindly provided by P.Ramage (Novartis AG, Basel, Switzerland).

Extraction of Myo5p and co-immunoprecipitation with Cmd1p

Extraction of Myo5p and co-immunoprecipitation experiments were performed based on Swanljung-Collins and Collins (1991) and Brockerhoff *et al*. (1994). Cells bearing the plasmids with myc-tagged wt or mutant *MYO5* were grown to a density of 2×10^7 cells/ml. 3×10^9 cells were used for each immunoprecipitation. Cells were harvested in 50 ml Falcon tubes and resuspended in 300 µl of buffer A (10 mM Imidazole–Cl, 4 mM EDTA, 1 mM EGTA, 0.02% NaN_3, 0.5 mM PMSF, 1 µg/ml aprotinin, 1 µg/ml leupeptin, 1 µg/ml pepstatin pH 7.3) on ice. Cells were lysed using glass beads. Unbroken cells and debris were eliminated by centrifuging at 2500 *g* at 4°C for 5 min and the supernatants were transferred to 1.5 ml polyallomer microfuge tubes (Beckman Instruments). Further steps were carried out at 4°C. Samples were centrifuged at 100 000 g for 15 min, in a TL100 Beckman table top ultra-centrifuge in a TLA-100 rotor. The supernatant was discarded and the pellet washed again in 300 µl of buffer A. After a second centrifugation, the pellet was extracted twice with 100 µl of buffer B (10 mM Imidazole–Cl, 0.2 M KCl, 5 mM $MgCl_2$, 5mM ATP, 1 mM EGTA, 0.02% NaN_3, 0.5 mM PMSF, 1 µg/ml aprotinin, 1 µg/ml leupeptin, 1 µg/ml pepstatin pH 6.8) for solubilization of Myo5p by first resuspending the samples in buffer B and then centrifuging for 20 min at 100 000 *g*. Both supernatants were recovered and transferred to an Eppendorf tube. Each sample (200 µl) was incubated on ice with slow rocking, with α-Cmd1p or preimmune serum previously bound to protein A sepharose. For the immunoprecipitations in the presence of Ca^{2+}, $CaCl_2$ was added to a final concentration of 5 mM. After 2 h, the beads were collected and washed once with 200 µl of buffer B. The beads were then extracted in 30 µl of 2×SDS–PAGE sample buffer (Pellet). The supernatants (total 400 µl) were precipitated with 12.5% TCA, washed once with cold acetone and resuspended in 30 µl of 2×SDS–PAGE sample buffer (Supernatant). One-tenth of each sample was processed for detection of wt or mutant Cmd1p and the rest for detection of myc-tagged wt or mutant Myo5p as described above.

E.coli expression systems, calmodulin purification and overlay assay

His_6-tagged Cmd1p purification was performed using a Ni-NTA resin (Qiagen) following the protocols specified by the company. pQE11*CMD1* was transformed into M15[pREP4] (Villarejo and Zabin, 1974) and Cmd1p expression induced for 4 h in LB (Sambrook *et al*., 1989) 50 µg/ml ampicillin, 25 µg/ml kanamycin at an initial cell density of 0.7 OD_{600} units by adding isopropyl β-D-thiogalactopyranoside (IPTG) to a final concentration of 1 mM. A denaturing procedure was used to purify Cmd1p for antibody injection. 500 ml culture yielded ~7.5 mg of Cmd1p >95% pure as judged by SDS–PAGE and staining. ^{35}S-labeled Cmd1p was purified from *E.coli* cells expressing Cmd1p (Brockerhoff *et al*. 1992) after labeling an IPTG-induced culture (OD_{600} of 0.25–0.3) with 10 mCi of $^{35}SO_4^{2-}$ (Amersham Life Science). The peak fraction contained approximately 25 µM Cmd1p greater than 95% pure as judged by SDS–PAGE and staining with a specific activity of 60 c.p.m./femtomol.

The pGEX-2T plasmids were transformed into the SG13009[pRE4] strain (Gottesman *et al*., 1981) for expression of the GST–IQ fusions. Cells were grown in LB, 50 µg/ml ampicillin, 25 µg/ml kanamycin until the culture reached OD_{600} of 0.7–0.8. Expression of the different constructs was induced by adding IPTG to a final concentration of 1 mM. The cells were incubated for 4 h, harvested and lysed in 2×SDS–PAGE sample buffer. The amount of induced proteins was adjusted to approximately equal amounts for the overlay assay as judged by SDS–PAGE and Coomassie staining.

The overlay assay was performed based on Brockerhoff *et al*. (1992) with some modifications. The bacterial extracts bearing the GST–IQ fusion proteins were separated on SDS–PAGE and transferred to a nitrocellulose filter in 30 mM Tris-base, 240 mM glycine. Proteins were then partially renatured by washing in 20 mM MES pH 6.8, three times for 30 min at room temperature (RT). The membranes were blocked overnight at 4°C in 20 mM MES, 0.05% Tween-20, 3% BSA pH 6.8. Membranes were then washed once at RT with buffer G (0.2 M KCl, 5 mM $MgCl_2$, 1mM EGTA pH 6.8) and probed with 50 nM ^{35}S-labeled Cmd1p in buffer G for 2 h at RT. Membranes were washed three times in buffer G for 2 min, and three times for 10 min, air-dried and exposed to Kodak XAR X-ray films.

Two-hybrid techniques

The interaction trap two-hybrid system was used (Gyuris *et al*., 1993). Plasmids pEG202, pJG4-5, pRFHM-1 and pSH18-34 and the strain EGY48 were obtained from R.Brent (MGM, Boston). To measure β-galactosidase activity, EGY48 bearing the lexAop-lacZ reporter plasmid pSH18-34, was cotransformed with the appropriate pEG202- and pJG4-5-derived plasmids and streaked out on X-Gal (5-bromo-4-chloro-3-indolyl-β-D-galactopyranoside) containing SD/Gal/Raf-His-Trp-Ura plates [0.67% yeast nitrogen base (Difco), 7 g/l Na_2HPO_4, 3 g/l NaH_2PO_4, 2% galactose, 1% raffinose, 40 mg/ml leucine, 80 mg/l X-Gal (Sigma Chemicals Co.), 2% agar pH 7]. Pictures were taken after 3 days of growth at 24°C. At temperatures >30°C, all lexA–calmodulin fusions gave unspecific lacZ transcription. Expression of all the lexA–calmodulin fusion proteins was confirmed by immunoblotting using α-Cmd1p antibodies. pEG202*cmd1-228*, pEG202*cmd1-239* and pEG202*cmd1-250* unspecifically activated lacZ transcription already at 24°C. However, when liquid assays for β-galactosidase activity were performed according to Reynolds and Lundblad (1996), a significantly higher activity was detected in the corresponding strains bearing the pJG4-5*IQ1IQ2* plasmid than in those bearing the pJG4-5*IQ1*Δ*IQ2*Δ plasmid (not shown).

α-factor uptake assay

[^{35}S]α-factor uptake assays were performed as described by Dulic *et al*. (1991). For the *MYO5* strains, a pulse and chase protocol was used. For the ts calmodulin mutants, a continuous presence assay was used. Cells were incubated at 37°C for 10 min before addition of α-factor. The samples were processed as described above. The internalization rates were calculated as the percentage of counts internalized per min between 5 and 10 min (linear range). All uptake assays were performed at least twice and the mean and standard deviations calculated for each time point.

Acknowledgements

We thank members of the Riezman laboratory for discussion and K.D'Hondt, A.Alconada and S.K.Lemmon for critical reading of the manuscript. We are grateful to D.Botstein for sending the *cmd1* strains and plasmids, to R.Brent for sending the two-hybrid strains and plasmids and to T.N.Davis for sending α-Cmd1p antibodies. We acknowledge the technical assistance of N.Stern, T.Eberle, and T.Aust. This work was funded by the Canton Basel-Stadt and by a grant to H.R. from the Swiss National Science Foundation. M.I.G. was a recipient of an EMBO fellowship.

References

Brockerhoff,S.E., Edmonds,C.G. and Davis,T.N. (1992) Structural analysis of wild-type and mutant yeast calmodulins by limited proteolysis and electrospray ionization mass spectrometry. *Protein Sci*., **1**, 504-516.

Brockerhoff,S.E., Stevens,R.C. and Davis,T.N. (1994) The unconventional myosin, Myo2p, is a calmodulin target at sites of cell growth in *Saccharomyces cerevisiae. J. Cell Biol*., **124**, 315–323.

Bénédetti,H., Raths,S., Crausaz,F. and Riezman,H. (1994) The *END3* gene encodes a protein that is required for the internalization step of endocytosis and for actin cytoskeleton organization in yeast. *Mol. Biol. Cell*, **5**, 1023–1037.

Clore,G.M., Bax,A., Ikura,M. and Gronenborn,A.M. (1993) Structure of calmodulin-target peptide complexes. *Curr. Opin. Struct. Biol*., **3**, 838–845.

Collins,K., Sellers,J.R. and Matsudaira,P. (1990) Calmodulin dissociation regulates brush border myosin I (110-kD-calmodulin) mechanochemical activity *in vitro*. *J. Cell Biol*., **110**, 1137–1147.

Davis,T.N., Urdea,M.S., Masiarz,F.R. and Thorner,J. (1986) Isolation of the yeast calmodulin gene: calmodulin is an essential protein. *Cell*, **47**, 423–431.

Dulic,V., Egerton,M., Elguindi,I., Raths,S., Singer,B. and Riezman,H. (1991) Yeast endocytosis assays. *Methods Enzymol*., **194**, 697–710.

Dower,W.J., Miller,J.F. and Ragsdale,C.W. (1988) High efficiency transformation of *E.coli* by high voltage electroporation. *Nucleic Acids Res*., **16**, 6127–6145.

Edelman,A.M., Takio,K., Blumenthal,D.K., Hansen,R.S., Walsh,K.A., Titani,K. and Krebs,E.G. (1985) Characterization of the calmodulin-binding and catalytic domains in skeletal muscle myosin light-chain kinase. *J. Biol. Chem*., **260**, 11275–11285.

Evan,G.I., Lewis,G.K., Ramsay,G. and Bishop,J.M. (1985) Isolation of monoclonal antibodies specific for human c-myc proto-oncogene product. *Mol. Cell. Biol*., **5**, 3610–3616.

Geiser,J.R., van Tuinen,D., Brockerhoff,S.E., Neff,M.M. and Davis,T.N. (1991) Can calmodulin function without binding calcium? *Cell*, **65**, 949–959.

Geli,M.I. and Riezman,H. (1996) Role of type I myosins in receptor-mediated endocytosis in yeast. *Science*, **272**, 533–535.

Gietz,R.D. and Sugino,A. (1988) New yeast–*Escherichia coli* shuttle vectors constructed with *in vitro* mutagenized yeast genes lacking six-base pair restriction sites. *Gene*, **74**, 527–534.

Goodson,H.V. and Spudich,J.A. (1995) Identification and molecular characterization of a yeast myosin I. *Cell. Motility Cytoskeleton*, **30**, 73–84.

Goodson,H.V., Anderson,B.L., Warrick,H.M., Pon,L.A. and Spudich,J.A. (1996) Synthetic lethality screen identifies a novel yeast myosin I gene (*MYO5*): myosin I proteins are required for polarization of the actin cytoskeleton. *J. Cell Biol*., **133**, 1277–1291.

Gottesman,S., Halpern,E. and Trisler,P. (1981) Role of sulA and sulB in filamentation by lon mutants of *Escherichia coli* K-12. *J. Bacteriol*., **148**, 265–273.

Gyuris,J., Golemis,E., Chertkov,H. and Brent,R. (1993) Cdi1, a human G_1 and S phase protein phosphatase that associates with Cdk2. *Cell*, **75**, 791–803.

Hicke,L., Zanolari,B., Pypaert,M., Rohrer,J. and Riezman,H. (1997) Transport through the yeast endocytic pathway occurs through morphologically distinct compartments and requires an active secretory pathway and Sec18p/N-ethylmaleimide-sensitive fusion protein. *Mol. Biol. Cell*, **8**, 13–31.

Horvath,A. and H. Riezman (1994) Rapid protein extraction from yeast. *Yeast* 10, 1305–1310.

Ito,H., Fukuda,Y., Murata,K. and Kimura,A. (1983) Transformation of intact yeast cells treated with alkali cations. *J. Bacteriol*., **153**, 163–168.

James,P.H., Vorherr,T., Krebs,J., Morelli,A., Castello,G., McCormick,D.J., Penniston,J.T., De Flora,A. and Carafoli E. (1989) Modulation of erythrocyte Ca^{2+}-ATPase by selective calpain cleavage of the calmodulin-binding domain. *J. Biol. Chem*., **264**, 8289–8296.

James,P.H., Vorherr,T. and Carafoli,E. (1995) Calmodulin-binding domains: just two faced or multi-faceted?. *Trends Biochem. Sci*., **20**, 38–42.

Janmey,P.A. (1994) Phosphoinositides and calcium as regulators of cellular actin assembly and disassembly. *Annu. Rev. Physiol*., **56**, 169–191.

Jung,G., Wu,X. and Hammer,J.A.,III (1996) *Dictyostelium* mutants lacking multiple classic myosin I isoforms reveal combinations of shared and distinct functions. *J. Cell Biol*., **133**, 305–323.

Karess,R.E., Chang,X.-J., Edwards,K.A., Kulkarni,S., Aguilera,I. and Kiehart,D.P. (1991) The regulatory light-chain of nonmuscle myosin is encoded by spaghetti-squash, a gene required for cytokinesis in *Drosophila*. *Cell*, **65**, 1177–1189.

Klee,C.B., Crouch,T.H. and Richman,P.G. (1980) Calmodulin. *Annu. Rev. Biochem*., **49**, 489–515.

Korn,E.D. and Hammer,J.A.,III (1990) Myosin I. *Curr. Opin. Cell Biol*., **2**, 57–61.

Kübler,E. and Riezman,H. (1993) Actin and fimbrin are required for the internalization step of endocytosis in yeast. *EMBO J*., **12**, 2855–2862.

Kübler,E., Schimmöller,F. and Riezman,H. (1994) Calcium-independent calmodulin requirement for endocytosis in yeast. *EMBO J*., **13**, 5539–5546.

Laemmli,U.K. (1970) Cleavage of structural proteins during the assembly of the head of bacteriophage T4. *Nature* (*Lond.*), **227**, 680–685.

Lamaze,C., Fujimoto,L.M., Yin,H.L. and Schmid,S.L. (1997) The actin cytoskeleton is required for receptor-mediated endocytosis in mammalian cells. *J. Biol. Chem.*, **272**, 20332–20335.

Maruta,H., Gadasi,H., Collins,J.H. and Korn,E.D. (1978) The isolated heavy chain of an *Acanthamoeba* myosin contains full enzymatic activity. *J. Biol. Chem*., **253**, 6297–6300.

Mooseker,M.S. and Cheney,R.E. (1995) Unconventional myosins. *Annu. Rev. Cell Dev. Biol*., **11**, 633–675.

Munn,A.L., Stevenson,B.J., Geli,M.I. and Riezman,H. (1995). *end5*, *end6*, and *end7*: mutations that cause actin delocalization and block the internalization step of endocytosis in *Saccharomyces cerevisiae*. *Mol. Biol. Cell*, **6**, 1721–1742.

Novak,K.D., Peterson,M.D., Reedy,M.C. and Titus,M.A. (1995) *Dictyostelium* myosin I double mutants exhibit conditional defects in pinocytosis. *J. Cell Biol*., 131, 1205–1221.

Ohya,Y. and Botstein,D. (1994a) Diverse essential functions revealed by complementing yeast calmodulin mutants. *Science*, **263**, 963–966.

Ohya,Y. and Botstein,D. (1994b) Structure-based systematic isolation of conditional-lethal mutations in the single yeast calmodulin gene. *Genetics*, **138**, 1041–1054.

Pley,U.M., Alibert,C., Brodsky,F.M. and Parham,P. (1995) The interaction of calmodulin with clathrin-coated vesicles, triskelions, and light-chains. Localization of a binding site. *J. Biol. Chem*., **270**, 2395–2402.

Pollard,T.D., Doberstein,S.K. and Zot,H.G. (1991) Myosin-I. *Annu. Rev. Physiol*., **53**, 653–681.

Raths,S., Rohrer,J., Crausaz,F. and Riezman,H. (1993) *end3* and *end4*: two mutants defective in receptor-mediated and fluid-phase endocytosis in *Saccharomyces cerevisiae*. *J. Cell Biol*., **120**, 55–65.

Reynolds,A., Lundblad,V., Dorris,D. and Keaveney,M. (1997) Yeast vectors and assays for expression of cloned genes. In *Current Protocols in Molecular Biology*, Volume II. John Wiley and Sons Inc., USA, 13.6.1–13.6.6.

Riezman,H., Munn,A., Geli,M.I. and Hicke,L. (1996) Actin-, myosin- and ubiquitin-dependent endocytosis. *Experientia*, **52**, 1033–1041.

Ruden,D.M., Ma,J., Li,Y., Wood,K. and Ptashne,M. (1991) Generating yeast transcriptional activators containing no yeast protein sequences. *Nature*, **350**, 250–252.

Salisbury,J.L., Condeelis,J.S. and Satir,P. (1980) Role of coated vesicles, microfilaments, and calmodulin in receptor-mediated endocytosis by cultured B lymphoblastoid cells. *J. Cell Biol*., **87**, 132–141.

Sambrook,J., Fritsch,E.F. and Maniatis,T. (1989) *Molecular Cloning: A Laboratory Manual*, *2nd ed*., Cold Spring Harbor Laboratory Press, Cold Spring Harbor, NY.

Sherman,S., Fink,G. and Lawrence,C. (1974) *Methods in Yeast Genetics*. Cold Spring Harbor Laboratory Press, Cold Spring Harbor, NY.

Sikorski,R.S. and Hieter,P. (1989) A system of shuttle vectors and yeast host strains designed for efficient manipulation of DNA in *Saccharomyces cerevisiae*. *Genetics*, **122**, 19–27.

Stöffler,H.-E., Ruppert,C., Reinhard,J. and Bähler,M. (1995) A novel mammalian myosin I from rat with an SH3 domain localizes to con A-inducible, F-actin-rich structures at cell–cell contacts. *J. Cell Biol*., **129**, 819–830.

Stotz,A. and Linder,P. (1990) The *ADE2* gene from *Saccharomyces cerevisiae*: sequence and new vectors. *Gene*, **95**, 91–98.

Swanljung-Collins,H. and Collins,J.H. (1991) Rapid, high-yield purification of intestinal Brush Border Myosin I. *Methods Enzymol*., **196**, 3–11.

Tan,J.L., Ravid,S. and Spudich,J.A. (1992) Control of nonmuscle myosins by phosphorylation. *Annu. Rev. Biochem*., **61**, 721–759.

Tang,H.-Y., Munn,A. and Cai,M. (1997) EH domain proteins Pan1p and End3p are components of a complex that plays a dual role in organization of the cortical actin cytoskeleton and endocytosis in *Saccharomyces cerevisiae*. *Mol. Cell. Biol*., **17**, 4294–4304.

Titus,M.A. (1997) Unconventional myosins: new frontiers in actin-based motors. *Trends Cell Biol*., **7**, 119–123.

Uyeda,T.Q.P. and Spudich,J.A. (1993) A functional recombinant myosin II lacking a regulatory light-chain-binding site. *Science*. **262**, 1867–1869.

Vale,R.D., Szent-Gyorgyi,A.G. and Sheetz,M.P. (1984) Movement of scallop myosin on *Nitella* actin filaments: regulation by calcium. *Proc. Natl Acad. Sci. USA*, **81**, 6775–6778.

Villarejo,M.R. and Zabin,I. (1974) Betα-galactosidase from termination and deletion mutant strains. *J. Bacteriol*., **120**, 466–474.

Wang,Z.Y., Sakai,J., Matsudaria,P.T., Baines,I.C., Sellers,J.R., Hammer,J.A.,III and Korn,E.D. (1997) The amino acid sequence of the light-chain of *Acanthamoeba* myosin Ic. *J. Muscle Res. Cell Motil*., **18**, 395–398.

Warmke,J., Yamakawa,M., Molloy,J., Fankenthal,S. and Maughan,D. (1992) Myosin light-chain-2 mutation affects flight, wing beat frequency, and indirect flight muscle contraction kinetics in *Drosophila*. *J. Cell Biol*., **119**, 1523–1189.

Wendland,B., McCaffery,J.M., Xiao,Q. and Emr,S.D. (1996) A novel fluorescence-activated cell sorter-based screen for yeast endocytosis

mutants identifies a yeast homologue of mammalian eps15. *J. Cell Biol*., **135**, 1485–1500.

Wesp,A., Hicke,L., Palecek,J., Lombardi,R., Aust,T., Munn,L.A. and Riezman,H. (1997) End4/Sla2p interacts with actin-associated proteins for endocytosis in *Saccharomyces cerevisiae*. *Mol. Biol. Cell*, **8**, 2291–2306.

Wolenski,J.S., Hayden,S.M., Forscher,P. and Mooseker,M.S. (1993) Calcium-calmodulin and regulation of brush border myosin-I Mg-ATPase and mechanochemistry. *J. Cell Biol*., **122**, 613–621.

Wolenski,J.S. (1995) Regulation of calmodulin binding myosins. *Trends Cell Biol*., **5**, 310–316.

Zurini,M., Krebs,J., Penniston,J.T. and Carafoli,E. (1984). Controlled proteolysis of the purified Ca^{2+}-ATPase of the erythrocyte membrane. A correlation between the structure and the function of the enzyme. *J. Biol. Chem*. **259**, 618–624.

Received September 30, 1997; revised November 18, 1997; accepted November 26, 1997